

MR BASED ATTENUATION CORRECTION INCLUDING CORTICAL BONE FOR PET/MR HYBRID IMAGING

Bharath K. Navalpakkam¹, Harald Braun², Joachim Hornegger¹, Torsten Kuwert³, and Harald H. Quick²

¹Pattern Recognition Lab, Friedrich-Alexander-University Erlangen-Nürnberg, Erlangen, Bavaria, Germany, ²Institute of Medical Physics, Friedrich-Alexander-University Erlangen-Nürnberg, Erlangen, Bavaria, Germany, ³Clinic of Nuclear Medicine, Friedrich-Alexander-University Erlangen-Nürnberg, Erlangen, Bavaria, Germany

Target audience: Researchers and physicians who are working in the new field of PET/MR hybrid imaging.

Introduction: Existing attenuation maps (μ -maps) for PET/MR systems discard the inclusion of cortical bone due the inherent difficulty in its detection from MR sequences. However, this causes an underestimation of attenuation towards ¹⁸F-DG-PET quantification [1, 2]. Ultrashort Echo Time (UTE) sequences have been used by many groups to differentiate cortical bone voxels from others [2, 3]. In this study, an MR based μ -map generation from UTE and 3D Dixon-VIBE sequences for the head region using pattern recognition methods is investigated based on model training on five patients. The generated μ -maps are evaluated on a different set of five patients not included in the training process and their respective PET quantification differences are reported. Further, initial results on the extension of the proposed method to whole-body regions are presented.

Methods: 10 patients were injected with ¹⁸F-FDG and scanned on a PET/CT (Biograph 64, Siemens Healthcare Sector, Erlangen, Germany) followed by a PET/MR (Biograph mMR, Siemens). Both UTE and 3D Dixon-VIBE sequences were acquired for each patient. Based on a prior work, an epsilon insensitive Support Vector Regression method is used to learn the mapping between the MR and CT intensities for fat, water and cortical bone classes [4]. The reason for using regression over a 4-class classification approach (air, fat, water, bone) is because the bone densities vary vastly for the head regions (300-2000 Hounsfield Units) and hence may not be well approximated by a single Linear Attenuation Coefficient (LAC) value. As kernel, a Radial Basis Function was used to project the input data to a higher dimensional feature space. The training and validation in this study was based on a larger patient collective (n=5). Four attenuation maps with assigned LACs were compared: 1) μ -map_{nobone} (air: 0 cm⁻¹, fat: 0.0854 cm⁻¹ and water: 0.1000 cm⁻¹), 2) μ -map_{bone} (air: 0 cm⁻¹, fat: 0.0854 cm⁻¹, water: 0.1000 cm⁻¹ and cortical bone: 0.1510 cm⁻¹), 3) μ -map_{MR} (continuous LACs) and 4) μ -map_{CT} (continuous LACs). The PET emission data was reconstructed (PET_{noboneAC}, PET_{boneAC}, PET_{MR} and PET_{CT}) from each of these μ -maps. For all reconstructed PET results, a Relative Difference (RD) image is computed against PET_{CTAC} as the reference. The segmentations from the complete brain and 13 anatomical landmarks close to cortical bone were analyzed for global and local PET quantification differences, respectively. A linear regression analysis was done using the relation $y = \alpha + \beta x$, where y and x represent the activities from PET_{CTAC} and PET_{MRAC}/PET_{noboneAC}/PET_{boneAC} respectively. Further, the generated model is applied on volunteer scans with the same set of MR sequences (UTE/3D Dixon-VIBE), without any injected radioactivity. A limitation for whole-body application however is the non-adjustable FOV which is currently optimized for head imaging with a maximum FOV of 300 x 300 mm².

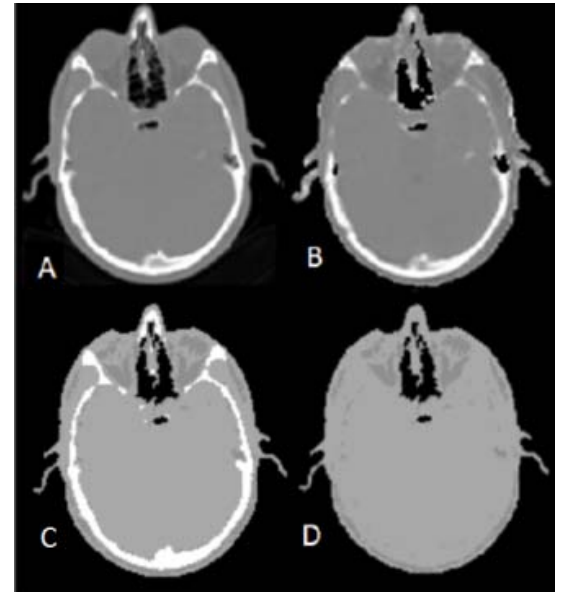


Figure 1: Compared μ -maps: (A): μ -map_{CT}, (B): μ -map_{MR}, (C): μ -map_{bone}, (D): μ -map_{nobone}. μ -map_{MR} closely resembles μ -map_{CT} than any other μ -map.

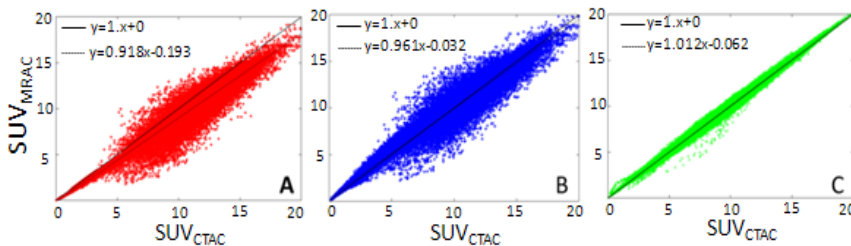


Figure 3: Scatter plots for (A) PET_{noboneAC}, (B) PET_{boneAC} and (C) PET_{MRAC}. PET_{MRAC} has a closer to identity slope than the other two methods. The coefficients of determination (R^2) for PET_{noboneAC}, PET_{boneAC} and PET_{MRAC} were 0.972, 0.961 and 0.994, respectively.

Results: A comparison of μ -maps is shown in Fig. 1. Global differences on PET from the investigated μ -maps are illustrated in Fig. 2. The mean absolute errors for PET_{noboneAC}, PET_{boneAC} and PET_{MRAC}, for the complete brain across five patients were 10.15±3.31 %, 3.96±3.71 % and 2.40±3.59 %, while on atlas segmented landmarks close to the cortical bone, the errors were 11.03±2.26 %, 4.22±3.91 %, and 2.16±1.77 %, respectively. Fig. 3 (A-C) shows the results of the linear regression analysis with slopes of 0.918, 0.961 and 1.012 for PET_{noboneAC}, PET_{boneAC} and PET_{MRAC}. Fig. 4 (A, B) shows an MR-based pseudo-CT for the abdominal region of a volunteer.

Discussion: In this study, PET quantification differences from the proposed method against other μ -maps (μ -map_{bone}, μ -map_{nobone}, and μ -map_{CT}) are evaluated. Further, an extension to whole-body μ -map prediction is shown using a limited FOV UTE (300 x 300 mm²).

Conclusion: The proposed method with continuous LACs estimates PET activities within a 3% error range compared to other methods in which the cortical bone was ignored (>10%) or included retrospectively (<4%) via a segmentation based approach.

References: [1] Samarin et al., Eur J Nucl Med Mol Imaging. 2012;39:1154-1160. [2] Catana et al., J Nucl Med. 2010; 51:1431-1438. [3] Keereman et al., J Nucl Med. 2010;51:812-818. [4] Krishnan Bharath et al., ISMRM, 2012.

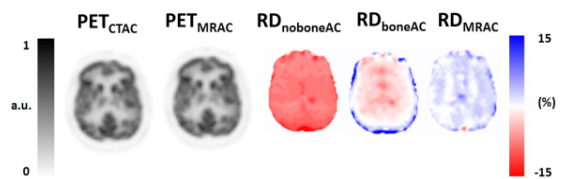


Figure 2: Attenuation corrected PET for the complete brain using μ -maps from Fig. 1. The proposed method reduces the bias at the skull periphery due to continuous LAC estimations.

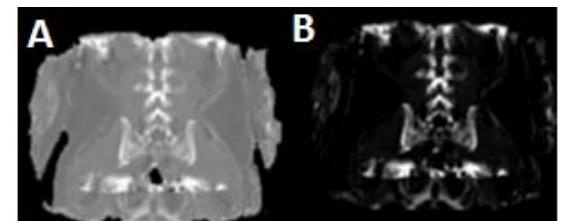


Figure 4: (A) Predicted MR based pseudo-CT using the limited FOV UTE. (B) window level adjusted to visualize bones. A distinction between bone and other tissue groups is visible.